THE EFFECT OF STRAIN ON INTRA- AND INTERLAYER MASS TRANSPORT IN METAL EPITAXY

H. BRUNE, K. BROMANN, and K. KERN
Institut de Physique Expérimentale, EPFL, CH-1015 Lausanne, Switzerland

ABSTRACT

A general concept is shown how to measure both the barriers for terrace and step-down diffusion for an epitaxial system. It is based on the application of mean-field nucleation theory to variable temperature STM data. With this approach we studied the influence of strain on intra- and interlayer diffusion for Ag self diffusion on strained and unstrained Ag(111) surfaces. The strained surface was the first Ag layer that grows pseudomorphically on Pt(111) and is thus under 4.2% compressive strain. The barrier for terrace diffusion is observed to be substantially lower on the strained, compared to the unstrained Ag/Ag(111) case, 60±10 meV and 97±10 meV, respectively. The additional barrier for interlayer diffusion decreases from 120±15 meV for Ag(111) homoepitaxy to only 30±5 meV for diffusion from the strained Ag layer down to the Pt(111) substrate. These examples illustrate the considerable effect of strain on the intra- and interlayer mass transport. They require a new concept of layer dependent nucleation kinetics for heteroepitaxial systems in general.

INTRODUCTION

The ultimate goal in epitaxial growth is the controlled fabrication of atomically thin films with smooth and abrupt interfaces. In the thermodynamic limit the growth morphology is determined by the balance of the surface and interfacial energies involved **[1]**. In most cases, however, thin films are grown under experimental conditions far from equilibrium. Film growth and the resulting morphology will then be governed by kinetic effects. The determining parameters entering in the kinetic regime are the energy barrier for surface (intralayer) diffusion and the additional energy barrier encountered by an adatom that descends an atomic step (interlayer diffusion) **[2, 3]**. The first determines the mean free path of a diffusing adatom on terraces and on-top of islands which build up during deposition. It decides whether and how often an adatom can visit the island edge. The second describes the average number of attempts necessary until an adatom descends the edge. It is the interplay of these two parameters that largely determines the film morphology. If atoms nucleate without having visited the island edge at all, or after they have visited it too few times to descend, 3D growth occurs. Otherwise, they are able to descend rapidly enough so that the critical density for nucleation never builds up on-top of islands and the film grows 2D.

In homoepitaxial systems, if no reconstructions are involved, both intra- and interlayer barriers remain unchanged with film thickness. In that case the mean free path on-top of islands is comparable to the island distance, which equals their maximum size before coalescence. Hence, each atom visits the island edges at least once and the only parameter that determines the film morphology is the barrier for interlayer diffusion.

In heteroepitaxial systems strain is involved. In addition the strain in the topmost layers, where nucleation occurs, changes with film thickness. Generally it is decreasing with increasing number of layers, since the film adopts more and more its bulk lattice constant as it grows thicker. Therefore it is obvious to ask whether strain influences the nucleation kinetics and, if it does, how the growth scenario will be modified. We will show here for the case of Ag/Pt(111) that surface and interlayer diffusion can strongly alter from layer to layer due to their different strain. In molecular dynamics simulations, it has been predicted for As/GaAs(110) and Si/Si(001) that strain should affect diffusion barriers **[4-6]**. We present the first experimental evidence for this effect observed for isotropic strain in metal epitaxy.

The method applied to measure surface migration barriers consists in the application of nucleation theory **[7, 8]** to saturation island densities obtained from STM as a function of deposition temperature **[9, 10]**. The analysis is done for a critical nucleus size of one, i.e., at temperatures where dimers are stable. In this case, it directly yields the activation energy (and attempt frequency) for surface migration, without requiring additional parameters like cluster

Mat. Res. Soc. Symp. Proc. Vol. 399 © 1996 Materials Research Society

binding energies **[9]**. The additional barrier for interlayer diffusion can be measured by studying the nucleation probability on-top of preexistent islands as a function of their size **[11, 12]** which will be illustrated below.

EXPERIMENT

The experiments were performed with a variable-temperature STM (25 K-800 K) operating in UHV **[13]**. The Ag films on Pt(111) are prepared by deposition of Ag at 450 K from an MBE Knudsen-cell at a background pressure better than $2x10^{-10}$ mbar and subsequent annealing to 800 K. As a strained surface we use the first Ag monolayer which grows pseudomorphically and is thus under 4.2% compressive strain **[14]**. In order to prepare an unstrained Ag(111) substrate we took advantage of the fact that very thick Ag films (>40 ML) grown on Pt(111) adopt the Ag(111) interplanar lattice constant and symmetry as characterized by He-diffraction **[15]**. STM images revealed that both, the pseudomorphic Ag layer on Pt(111), and the Ag(111) surface consisted of extended flat terraces which were free of dislocations. For the study of nucleation kinetics, submonolayer coverages have been deposited (flux $1.1x10^{-3}$ ML/s) onto these layers at various temperatures. Island densities are given in islands per Pt substrate atom, i.e., in ML. They were obtained on extended terraces to exclude the influence of steps and corrected for lateral drift.

RESULTS

A strong layer dependence of island densities becomes evident from inspection of Figure 1. It shows nucleation on the Pt(111) substrate (a), the first (b) and second (c) Ag layer, as well as on a 50ML thick Ag layer which has adopted Ag(111) geometry (d). In all cases, except Fig. 1c) (see below), the island density has saturated. These saturation island densities can be related to diffusion based on the following nucleation scenario. At the beginning of deposition the density of nuclei steadily increases as a function of coverage until it becomes more probable that diffusing atoms attach to existing islands rather than create new ones. At this state the island density stays nearly constant in a wide coverage range of Θ = 0.05 - 0.20 ML until it eventually decreases due to coalescence. Its maximum, the saturation island density, is determined by the ratio of the diffusivity to the deposition flux and therefore a measure for the adatom mobility at known deposition flux **[8]**. It is important to note that nucleation of islands takes place at the time of deposition. After deposition, nucleation is then terminated and the resulting island density is stationary under isothermal conditions where it has been imaged by STM.

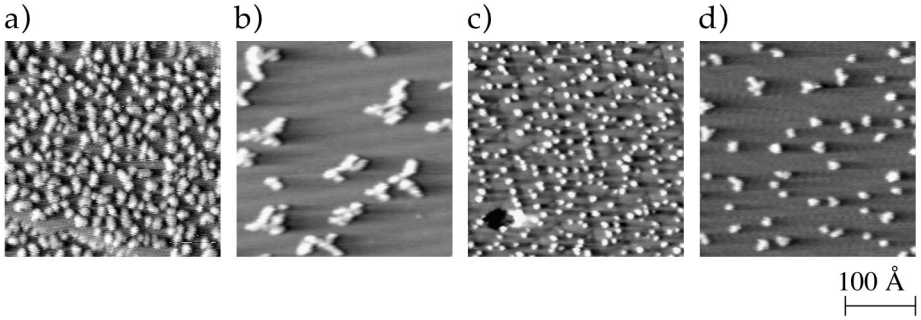

Fig. 1: STM images showing the nucleation of submonolayer coverages of Ag on Pt(111) (a), on 1MLAg/Pt(111) (b), on 2MLAg/Pt(111) (c), and, on Ag(111) (d), respectively ((a) saturation island density $N_x = 1.7x10^{-2}$ islands per Pt(111) surface atom, Θ = 0.12 ML, (b) $N_x = 6.6x10^{-4}$, Θ = 0.05 ML, (c) $N = 1.6x10^{-2}$, Θ = 0.03 ML (note that the mean island size Θ/N is 2, i.e. saturation is not yet reached for this case), (d) $N_x = 3.8x10^{-3}$, Θ = 0.03 ML, (a) and (b) temperature of deposition and STM measurement T = 65 K, (c) and (d) T = 60 K, for all images: deposition flux $R = 1.1x10^{-3}$ MLs^{-1}, size 307x307 $Å^2$).

The island density shows an oscillatory behavior with layer thickness. It decreases by a factor of 26 when going from the Pt substrate to the pseudomorphic first Ag layer. The density then attains again the substrate value on the second layer. In this discommensurate layer the strain is relieved in a trigonal dislocation network which becomes visible in the STM image as dark lines that include small triangles where they cross **[14]**. Note that in Figure 1c) the island density is not yet at saturation, which implies an even higher saturation density, i. e., lower mobility than suggested from the figure. Nucleation on Ag(111) finally leads again to a slight decrease in island density (see Fig.1d). Already from this set of STM images, depicted at 60 K - 65 K, a strong influence of layer thickness on the adatom mobilities can be concluded.

In order to quantify the parameters for surface diffusion of Ag on these layers, we have measured the saturation island density as a function of temperature for the three cases of an isotropic substrate. The results are shown in Arrhenius representation in Fig. 2. For Ag on Pt(111) it has recently been demonstrated that application of mean-field nucleation theory **[8]** yields reliable information on the energy barrier and prefactor for surface diffusion (E_m = 157±10 meV, $\nu_0 = 1x10^{13\pm0.4}$ s^{-1}) **[9]**. With these values the experimental island densities are exactly reproduced for all temperatures investigated, either upon integration of rate equations **[9]**, or by kinetic Monte Carlo simulations with these parameters (we applied the same Monte-Carlo code as in ref. **[16]**). This gives us confidence in applying the same procedure also to the two other cases, i.e. Ag/1MLAg/Pt(111) and Ag/Ag(111). They equally show an Arrhenius behavior of the saturation island density (see Fig. 2). Annealing experiments as well as the absence of sharp bends in $\log N_x$ vs. (1/T) plots **[9]** show that dimers are stable (and immobile) in all three cases for the temperatures for which island densities are shown in Fig. 2.

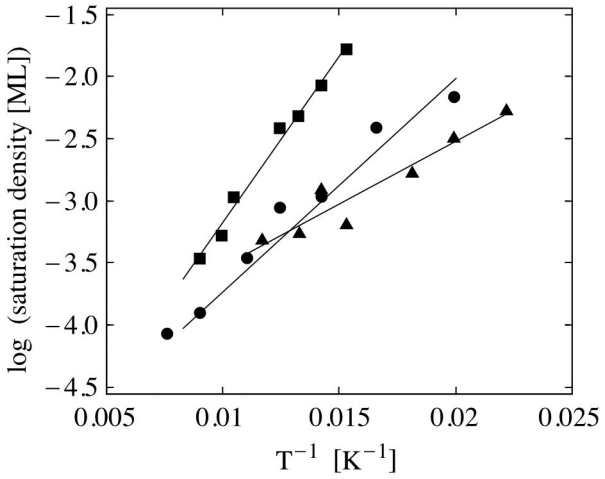

Fig. 2: Arrhenius plot of saturation island densities derived from STM for nucleation of Ag on Pt(111) (■), on 1MLAg adsorbed on Pt(111) (4.2% strain) (▲), and on Ag(111) (●), respectively.

For Ag diffusion on the isotropically strained first layer on Pt(111) we find a migration barrier of E_m = 60±10 meV from the slope of the line fit and from its intersection with the ordinate $\nu_0 = 1x10^{9\pm0.6}$ s^{-1}. Compared to the substrate this is a rather low barrier which explains the drastic decrease in island density at 65 K evident from Fig. 1b). For Ag self diffusion on Ag(111), on the other hand, we obtain E_m = 97±10 meV for the diffusion barrier with the corresponding attempt frequency of $\nu_0 = 2x10^{11\pm0.5}$ s^{-1} **[17]**. Therefore at low temperature, where the activation energy dominates the diffusion rate, the island density on the thick Ag(111) layer is in between that on the first layer and on the Pt substrate (see Fig. 1d). Note that with the change in barriers also a change in prefactor can go hand in hand. From Fig. 2 it is seen that this leads to crossing at T = 85 K. From this temperature on, the ratio of island densities of the strained and unstrained case is inverted.

The lowering of the surface migration barrier by 40% on the pseudomorphic Ag layer with respect to that on Ag(111) is remarkable. It is difficult to decide *a-priori* whether strain or the electronic adlayer-substrate coupling are causing this effect. We have recently studied the influence of lattice strain and electronic adlayer-substrate coupling for the Ag/Pt(111) system by calculations with effective medium theory **[18]**. In these calculations, strain effects clearly dominate the electronic adlayer-substrate coupling. Actually, it turned out that the electronic coupling even weekend the effect, as the diffusion barrier for a 4% compressed Ag-slab was found to be even lower than that of the pseudomorphic monolayer on Pt(111). The change in diffusion barrier, evident from Fig. 2, can thus clearly be attributed to strain.

For nucleation of Ag on a regular array of dislocations, we see from Fig. 1c) that the island density is strongly increased with respect to the unstrained and the homogeneously strained case. Further, we find that only few of the nuclei form directly on dislocations. For increasing temperature, nucleation substantially differs from that on isotropic surfaces. The island density asymptotically approaches a minimum at 110K, where on the average one island forms per unit cell of the dislocation network. From this we conclude that the dislocations constitute a rather effective repulsive barrier for adatoms that confines them to the pseudomorphic domains. At higher temperatures this confinement artificially increases the island density even if diffusion on the homogeneously strained parts of the surface may be fast. A similar effect has recently been observed for Ni nucleation on the dislocation network and moiré structures formed by Ni on Ru(0001) **[19]**.

The barriers for interlayer diffusion have been measured based on the following idea which was first put forward by Tersoff et al. **[11]**. Application of mean-field nucleation theory to calculate the nucleation probability on-top of an island yields a sharp transition from 0 to 1 at a certain island radius which depends on temperature. This can be exploited to extract the additional barrier for interlayer diffusion ΔE_S and its attempt frequency from a series of measurements of the nucleation probability on-top of preexistent islands as function of their size and substrate temperature at which the post-deposition is performed **[12]**. Islands with defined size can be prepared by two-dimensional Ostwald ripening, i.e. annealing of small islands until the mean island size has reached the desired value **[20]**. Fig. 3a) shows an example where 0.1ML Ag have been deposited at 40 K onto Pt(111) which predominantly created dimers. Afterwards, this surface was annealed to 230 K, which yielded compact islands of a mean size of 200 atoms. As can be seen the resulting size distribution is still sufficiently broad for the transition to be studied.

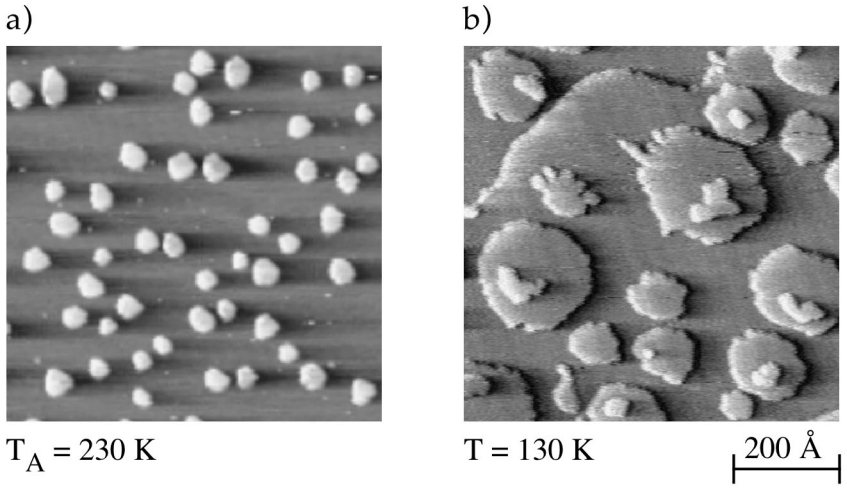

Fig. 3: (a) STM image illustrating the formation of 2D Ag islands on Pt(111) with defined sizes via deposition of 0.1 ML Ag at 40 K and subsequent annealing to 230 K (2D-Ostwald ripening). (b) STM image showing the result of the subsequent nucleation experiment, in which 0.1 ML Ag are deposited (flux = $1.1 \cdot 10^{-3}$ ML/s) at 130K on islands that were previously grown via Ostwald ripening on Ag(111).

Fig. 3b) shows that, after the second deposition, there are small islands where no nucleation occurs on-top and bigger ones where nucleation always occurs. This behavior has been studied quantitatively for three temperatures for Ag homoepitaxy and Ag nucleation on strained Ag islands adsorbed on Pt(111). Since the barriers and attempt frequencies for surface diffusion are known for both these cases, the only fit parameters are those for interlayer diffusion. An additional barrier of ΔE_S = 120±15 meV and attempt frequency of $\nu_s = 1x10^{13\pm1}$ s^{-1} are obtained for the interlayer diffusion in Ag homoepitaxy. Therefore an adatom has to overcome more than twice the barrier for terrace diffusion in order to descend at steps. This explains the fact that Ag(111) homoepitaxy is three-dimensional at temperatures below 400 K **[21]**. In a very recent analysis of the occupancy of open layers as a function of coverage, developed for homoepitaxy, Meyer et al. found ΔE_S = 150±20 meV for Ag/Ag(111) from experiments at 300 K **[19]**, which is in fair agreement with our result.

The activation energy for step-down diffusion in the heteroepitaxial system Ag/Ag-islands/Pt(111) is determined to ΔE_S = 30±5 meV ($\nu_s = 1x10^{9\pm1}$ s^{-1}). This is a rather small barrier which can easily be overcome. This is the reason for the perfect 2D growth of the first Ag monolayer on Pt(111) down to temperatures as low as 80 K. The influence in island shape, i.e. whether they are compact or ramified, is much less important since even on large compact islands, produced from Ostwald ripening, all Ag atoms post-deposited at 80 K can descend.

The strained pseudomorphic Ag islands on Pt(111) preferentially relieve their strain at the edges where the Ag atoms are more free to expand. This might cause a lowering in lateral binding energy of atoms at the island edge which in turn facilitates exchange processes. It is known that for several fcc (111) substrates exchange is, at least at B-steps, the dominant mechanism by which interlayer diffusion takes place **[16, 22]**. A second major difference to the homoepitaxial case is the different binding energy for an Ag adatom on the Pt(111) surface. While in homoepitaxy both, upper and lower terrace are energetically on the same level, in the case of Ag/Pt(111) the upper Ag terrace is about 170meV higher in energy than the lower Pt terrace, as inferred from thermal desorption experiments **[23]**. Both effects may bend the step potential close to the step edge accounting for the small additional step-edge barrier of the strained case compared to Ag(111).

Since we were able to measure the surface migration barriers on the terraces and at steps we have in a way mapped out the corrugation of the adsorption potential seen by a Ag adatom on a growing Ag film on Pt(111). The resulting potential energy diagrams are shown in Fig. 4, where (a) is for Ag(111) homoepitaxy and (b) for a Ag atom diffusing from the first strained Ag layer down to the Pt(111) substrate. The difference in binding energy in case (b) is from ref. **[23]**.

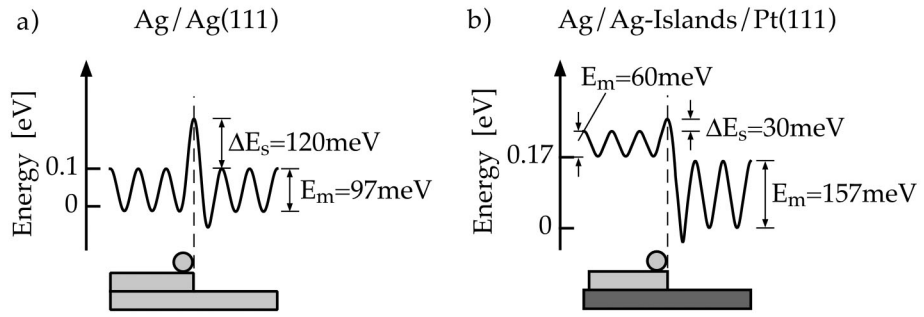

Fig. 4: Potential energy diagram characterizing the inter- and intralayer diffusion in Ag homo- (a) and heteroepitaxy (b) at the (111) surfaces of Ag and Pt.

CONCLUSIONS

We have applied mean-field nucleation theory to variable temperature STM data in order to measure the energy barriers and attempt frequencies for intra- and interlayer diffusion for Ag homoepitaxy and heteroepitaxy on the (111) surfaces of Ag and Pt. On the pseudomorphic Ag layer the barrier for terrace diffusion is lowered by 40% with respect to that on Ag(111). Similarly, the additional barrier for interlayer diffusion is substantially lower on the pseudomorphic layer compared to Ag(111) homoepitaxy. The effect seen for intralayer diffusion can unequivocally be attributed to the 4.2% compressive strain present in the pseudomorphic Ag layer on Pt(111). The low interlayer barrier for the strained system is likely to be as well an effect of strain which may facilitate exchange processes.

While it has been demonstrated for a particular model system that misfit strain can strongly alter barriers for intra- and interlayer diffusion, its implications for heteroepitaxial growth in the kinetic regime are of general significance. This implies a new concept of layer dependent adatom mobilities and island densities caused by strain which constitutes, together with the barrier for intralayer diffusion, an essential ingredient for the understanding and modeling of the kinetics of heteroepitaxial growth.

REFERENCES:

[1] E. Bauer, Z. Kristallogr. **110**, 372 (1958).
[2] G. Ehrlich and F. G. Hudda, J. Chem. Phys. **44**, 1039 (1966).
[3] R. L. Schwoebel and E. J. Shipsey, J. Appl. Phys. **37**, 3682 (1966).
[4] S. V. Ghaisas, Surf. Sci. **223**, 441 (1989).
[5] C. Roland and G. H. Gilmer, Phys. Rev. B **46**, 13428 (1992).
[6] H. Spjut and D. A. Faux, Surf. Sci. **306**, 233 (1994).
[7] J. A. Venables, Philos. Mag. **17**, 697 (1973).
[8] J. A. Venables, G. D. T. Spiller and M. Hanbücken, Rep. Prog. Phys. **47**, 399 (1984).
[9] H. Brune, H. Röder, C. Boragno and K. Kern, Phys. Rev. Lett. **73**, 1955 (1994).
[10] J. A. Stroscio and D. T. Pierce, Phys. Rev. B **49**, 8522 (1994).
[11] J. Tersoff, A. W. D. v. d. Gon and R. M. Tromp, Phys. Rev. Lett. **72**, 266 (1994).
[12] K. Bromann, H. Brune, H. Röder and K. Kern, Phys. Rev. Lett. **75**, 677 (1995).
[13] H. Brune, H. Röder, C. Romainczyk, C. Boragno and K. Kern, Appl. Phys. A **60**, 167 (1995).
[14] H. Brune, H. Röder, C. Boragno and K. Kern, Phys. Rev. B **49**, 2997 (1994).
[15] C. Romainczyk, M. Krzyzowski, P. Zeppenfeld, G. Comsa and K. Kern, to be published (1995).
[16] J. Jacobsen, K. W. Jacobsen, P. Stoltze and J. K. Nørskov, Phys. Rev. Lett. **74**, 2295 (1995).
[17] The error for E_m is predominantly due to scatter of the data. That for ν_0 comes from the uncertainty of $\eta(\Theta)$ in eq. (2.15) of ref. 8, (we assumed $\eta(\Theta_{saturation}) = 0.20 \pm 0.04$ see fig. 6c for i = 1 in that reference) and from the error in slope, i.e. in E_m.
[18] H. Brune, K. Bromann, H. Röder, K. Kern, J. Jacobsen, P. Stolze, K. Jacobsen and J. Nørskov, Phys. Rev. B in press (1995).
[19] J. A. Meyer, P. Schmid and R. J. Behm, Phys. Rev. Lett. **74**, 3864 (1995).
[20] H. Röder, E. Hahn, H. Brune, J. P. Bucher and K. Kern, Nature **366**, 141 (1993).
[21] H. A. v. d. Vegt, H. M. v. Pinxteren, M. Lohmeier, E. Vlieg and J. M. Thornton, Phys. Rev. Lett. **68**, 3335 (1992).
[22] S. C. Wang and G. Ehrlich, Phys. Rev. Lett. **75**, 2964 (1995).
[23] T. Härtel, U. Strüber and J. Küppers, Thin Sol. Films **229**, 163 (1993).